Journal of Geodynamics 144 (2021) 101816

Contents lists available at ScienceDirect

Journal of Geodynamics

journal homepage: www.elsevier.com/locate/jog

Eurekan faults on northern Ellesmere Island, Arctic Canada: from Cenozoic strike-slip tectonics to recent seismicity

Christian Brandes [a,*], Karsten Piepjohn [b]

[a] Institut für Geologie, Leibniz Universität Hannover, Callinstr. 30, 30167, Hannover, Germany
[b] Bundesanstalt für Geowissenschaften und Rohstoffe (BGR), Stilleweg 2, 30655, Hannover, Germany

ARTICLE INFO

Keywords:
Eurekan deformation
strike-slip tectonics
Ellesmere Island
Pearya Terrane
paleostress analsysis

ABSTRACT

The Eurekan deformation is a partially contractional Cenozoic tectonic event that affected large parts of the Arctic region. In the study area on northern Ellesmere Island, major NE-SW trending strike-slip faults occur, which are related to the Eurekan deformation. The outcrop data show that left-lateral strike-slip kinematics slightly dominate, but also right-lateral kinematics were documented. Cross-cutting relationships of the individual faults give evidence for multiple fault reactivations within major strike-slip zones. The reconstructed paleostress fields show two phases. The first phase started with a N-S compression and shifted over a NNE-SSW compression into a NNW-SSE compression. The second phase was a WNW-ESE compression. The paleostress field evolution reflects the movements of Greenland. During the Eurekan phase 1, Greenland moved northward and during Eurekan phase 2 it moved to the WNW. These motions likely controlled the stress field on northern Ellesmere Island. From the paleostress field analyses and the orientation of the strike-slip faults in the study area, it can be derived that the Eurekan phase 1 deformation is characterized by left-lateral strike-slip faults, whereas most-likely during Eurekan phase 2 the majority of right-lateral strike-slip faults formed. The paleostress field analysis implies that many Eurekan faults are reactivated Ellesmerian faults. Recent seismic events indicate ongoing tectonic activity at some of the major strike-slip faults. This sheds new light on the geodynamics of northern Ellesmere Island, which was mechanically coupled to the Greenland plate, and implies that under the recent stress field, earthquakes at strike-slip faults are still possible and some of these faults were active in at least three phases over the last 350 Myr.

1. Introduction

The Mesozoic-Cenozoic opening of the Arctic Ocean during the break-up of Laurasia is not yet completely understood (Arbeitskreis Geologie und Geophysik der Polargebiete der Deutschen Gesellschaft für Polarforschung (AGGP, 2015). In this context, the Paleogene Eurekan deformation is a major tectonic deformation phase that is directly related to the simultaneous opening of the Baffin Bay/Labrador seas, the North Atlantic Ocean and the Eurasia Basin (Tessensohn & Piepjohn, 2000; Piepjohn et al., 2016). The Pearya Terrane (Fig. 1) located at the northern margin of Ellesmere Island, represents a key element for understanding the geodynamic evolution of the Eurekan deformation. Recently, the geology of the Pearya Terrane was investigated in different studies, with a focus on geochronology and provenance (e.g., Malone, 2012; Hadlari et al., 2014; Dewing et al., 2019). The rift-related Cretaceous magmatism was studied by Estrada & Henjes-Kunst (2013). The faults on Ellesmere Island were analysed in different studies with a focus on the structural style and the fault kinematics (Trettin & Parrish, 1987; Estrada et al., 2006; von Gosen et al., 2012; McClelland et al., 2012; Piepjohn et al. 2008, 2013, 2016; Piepjohn & von Gosen, 2017). The crustal structure of the region has recently been investigated by Stephenson et al. (2017).

The Eurekan deformation was a contractional deformation event (Tessensohn & Piepjohn, 2000) that was also characterized by widespread strike-slip tectonics (Piepjohn et al., 2016). It attracted significant attention over the last years. Heron et al. (2015) carried out a numerical modelling study of the Eurekan deformation to explain the distribution of deformation across Ellesmere Island. A comprehensive overview of the Eurekan deformed belt covering Spitsbergen, North Greenland and the Canadian high Arctic was given by Piepjohn et al. (2016). In addition, Gion et al. (2017) presented a plate tectonic model for the Eurekan deformation. The Eurekan deformation took place in

* Corresponding author.
E-mail address: brandes@geowi.uni-hannover.de (C. Brandes).

https://doi.org/10.1016/j.jog.2021.101816
Received 24 February 2020; Received in revised form 7 January 2021; Accepted 15 January 2021
Available online 22 January 2021

two phases (phase 1 between 53-47 Ma and phase 2 between 47-34 Ma) (Piepjohn et al., 2000; Tessensohn & Piepjohn, 2000; Saalmann et al., 2005, 2008; Piepjohn et al., 2016; Gion et al., 2017). Previous work on the Eurekan deformation was also carried out by Lepvrier & Geyssant (1984) and Lepvrier (1990, 1992).

However, there are still open questions regarding the timing and the sequence of strike-slip fault activity, or the nature of the fault zones in the Nares Strait area. Therefore, this study focuses on strike-slip tectonics. We analysed Eurekan strike-slip faults within the western part of the Pearya Terrane and south of it on northern Ellesmere Island (Fig. 1) in order to derive the paleostress field of the region and to reconstruct the tectonic evolution of the area.

2. Geological setting

The northernmost part of Ellesmere Island is named Pearya (Schuchert, 1923) (Fig. 1) and interpreted as a composite terrane (Frisch, 1974; Churkin & Trexler, 1980) that was accreted to the margin of Laurentia in late Silurian times (Trettin, 1987) or in the earliest Carboniferous (Piepjohn et al., 2015). Following Trettin (1987), the Pearya Terrane can be subdivided into four successions (Fig. 1). Succession I represents a Proterozoic crystalline basement complex, composed of amphibolite grade metasedimentary and metavolcanic rocks, which were intruded by granites (Trettin, 1987; McClelland et al., 2012). Succession II covers carbonates and clastic sedimentary rocks, with minor intercalations of volcanic rocks, cherts and diamictites with depositional ages from Late Proterozoic to Late Cambrian/Early Ordovician. The Lower to Middle Ordovician Succession III comprises arc-derived volcanic rocks, cherts, mudstones and carbonates. Fault bounded slivers of ultramafic rocks probably represent remnants of ophiolites. Succession IV is an approximately 7-8 km thick unit of late Middle Ordovician to Late Silurian volcanic and sedimentary rocks (Trettin, 1987). Ellesmere Island has been affected by three tectonic events, the M′Clintock Orogeny, the Ellesmerian Orogeny and the Eurekan deformation. The M′Clintock Orogeny of the Pearya Terrane correlates with the Caledonian Orogeny on Svalbard. It took place around 452 Ma (Trettin, 1987) and at that time the translation of the Pearya Terrane toward the north Laurentian margin occurred in the early stages of the Baltica-Laurentia Caledonian collision (McClelland et al., 2012). The Ellesmerian Orogeny produced a large fold-and-thrust belt on Ellesmere Island southeast of the Pearya Terrane (Thorsteinsson & Tozer, 1970; Bjørnerud & Bradley, 1994; Piepjohn et al., 2008, 2013, 2015). The sedimentary successions of this area have been investigated by Beranek et al. (2015). Finally, the Eurekan deformation affected the entire area (Piepjohn et al., 2016).

The study area is dominated by rocks of Pearya Succession I and II (Fig. 1). The Petersen Bay Fault Zone represents the terrane boundary between the Pearya Terrane in the northwest and the Laurentian Neoproterozoic and Paleozoic Franklinian Basin and the Ellesmerian fold-and-thrust belt in the southeast (Fig. 1) (Trettin & Frisch, 1987, 1996; Klaper, 1992; Estrada et al. 2006; Piepjohn et al. 2013, 2016). Age control exists for magmatic rocks on the Pearya Terrane and the northern part of the Franklinian Basin (Estrada et al., 2006; Estrada & Henjes-Kunst, 2013) and a robust stratigraphic framework is established for the Paleozoic sedimentary units of the Franklinian Basin southeast of the Pearya Terrane (e.g., Trettin, 1987; Dewing et al. 2004, 2008, and citations therein).

3. Methods

The data of this study were collected during the CASE 19 expedition of the German Federal Institute for Geosciences and Natural Resources (BGR) in summer 2017 on northern Ellesmere Island (Fig. 1). Altogether 27 outcrops were analysed and in 14 of these outcrops, slickenside orientations were measured with a Freiberg compass. The outcrops cover the major fault zones such as the Petersen Bay Fault Zone (Figs. 2–4) and the Emma Fiord Fault Zone as well as minor faults in between. The slickenside measurements were used for fault-slip analyses with the software FaultKin and the P- and T-axes were calculated based on the approach shown in Marrett & Allmendinger (1990). From the P- and T- axis orientations, the directions of paleo-shortening and paleo-extension were derived. Such a paleostress field analysis allows estimating the past stresses that acted in the crust for a certain period of deformation, averaged over the duration of a tectonic event (Lacombe, 2012) and delivers information about the regional tectonic processes (e.g., Delvaux et al., 1997; Saintot and Angelier, 2002).

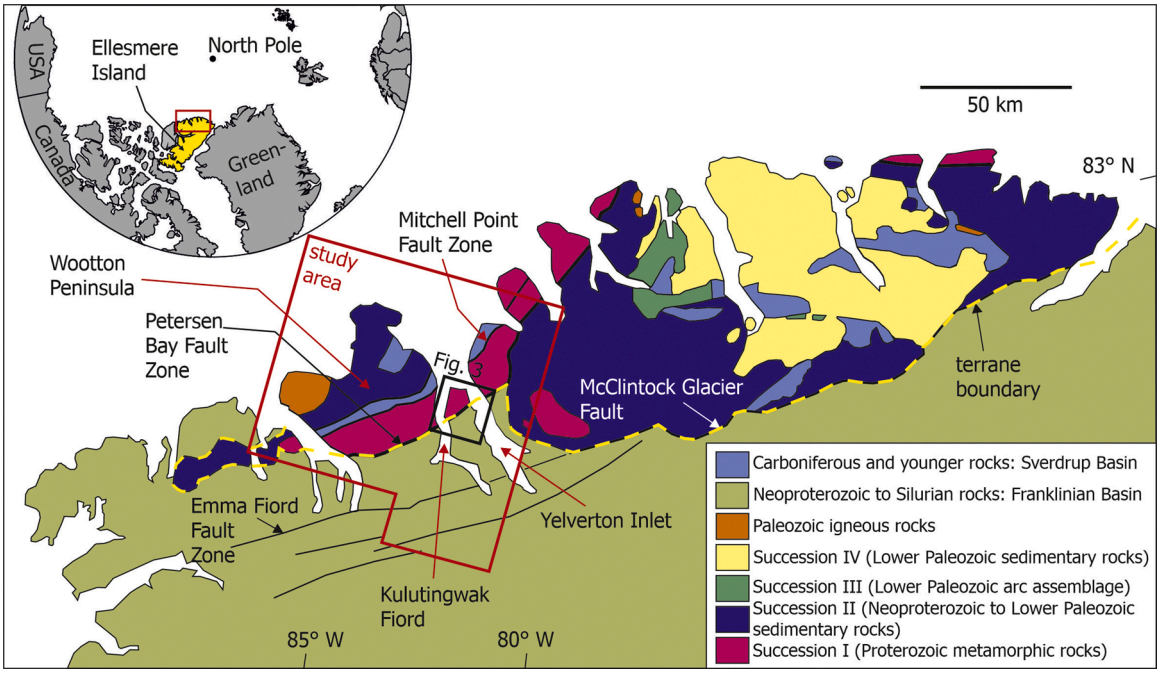

Fig. 1. Geological map of the Pearya Terrane, modified after Trettin (1991) and McClelland et al. (2012). The terrane boundary is shown as dashed yellow line. The red box indicates the study area. The black box indicates the location of Fig. 3.

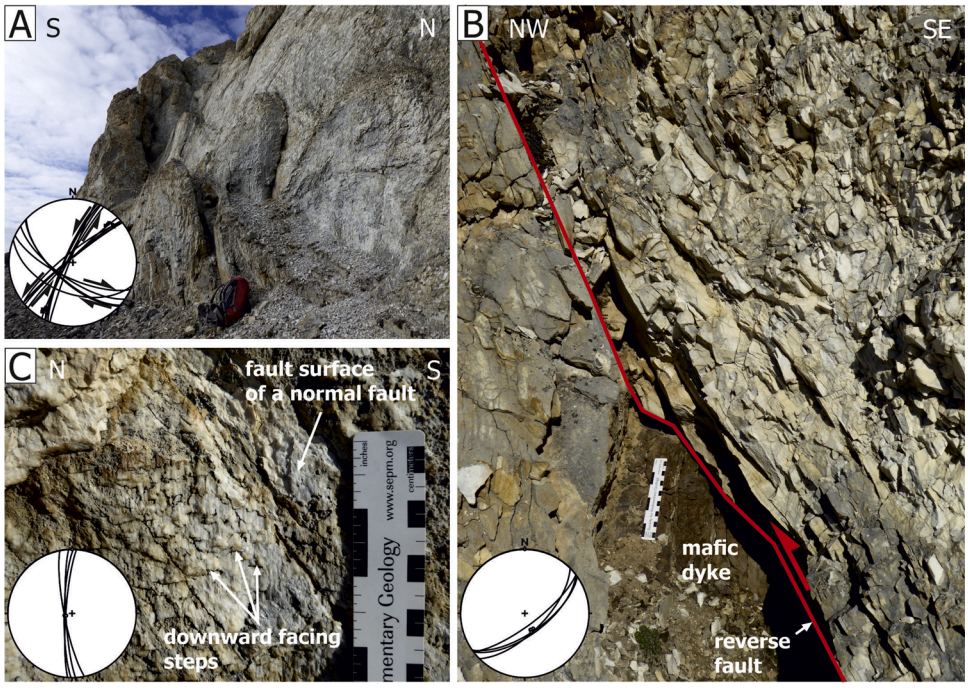

Fig. 2. Petersen Bay Fault Zone. A) Overview of the fault core that is characterized by fractured marble mylonites. The outcrop contains multiple slip surfaces that show slickensides and indicate left-lateral strike-slip movements. View is to the west. B) Reverse fault related to the Petersen Bay Fault Zone that offsets a mafic dyke. The dyke belongs to a system of dykes that is lower Cretaceous to Cenomanian in age (Estrada et al., 2006; Estrada & Henjes-Kunst, 2013) indicating a post-Cretaceous fault activity. C) Slickenside that indicates normal fault movements related to the Petersen Bay Fault Zone. View is onto the fault surface of the normal fault.

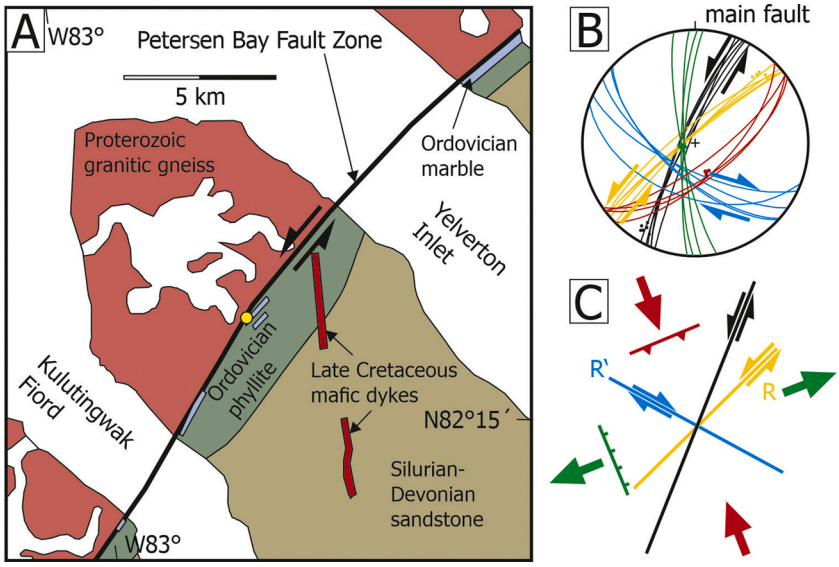

Fig. 3. Area between Yelverton Inlet and Kulutingwak Fiord. A) Geological map with the trace of the Petersen Bay Fault Zone (map is modified after Trettin & Frisch, 1996). B) Stereographic projection of individual faults in the area. Strike-slip faults are shown in black, yellow, and blue. Normal faults in green and reverse faults in red. C) Conceptual kinematic model for a strike-slip fault with Riedel and anti-Riedel shears and related normal and reverse faults (based on Wilcox et al., 1973; Christie-Blick & Biddle, 1985). The faults developed in the Petersen Bay Fault Zone shown in B), match to this conceptual model, which implies that they all formed during one deformation phase. For location see Fig. 1. The yellow dot indicates the location of the analysed outcrop at the Petersen Bay Fault.

4. Structural analysis

In four of the 27 analysed outcrops (three outcrops south of the Petersen Bay Fault Zone and one outcrop south of the Emma Fiord Fault Zone) fold data comprising fold axes, intersection lineations and the related foliation were measured. In 14 outcrops faults are exposed that delivered the necessary structural information (orientation of the fault surface, orientation and kinematics of the striations) for a fault analysis. Altogether 342 measurements were made (171 value pairs that contain a value for the fault surface orientation and a value for the orientation of the striation). For 155 value pairs it was possible to calculate P- and T-axes (see Table 1). There was no significant variation in the measured values at an individual fault in each outcrop, thus we took five to six value pairs at each fault. The outcrop conditions varied throughout the study area. A limited number of strongly weathered outcrops only allowed to take two to three measurements.

5. Results

5.1. Faults north and south of the Mitchell Point Fault Zone

The Mitchell Point Fault Zone is a NE-SW striking major fault zone located within the Pearya Terrane and runs through the central part of the Wootton Peninsula (Fig. 1, 4). In this study outcrops north and south of the Mitchell Point Fault Zone were analysed (see Table 1). Oblique reverse and normal faults occur, as well as right-lateral strike-slip faults are developed at the east coast of the Wootton Peninsula.

5.2. Petersen Bay Fault Zone

The Petersen Bay Fault Zone runs across the Wootton Peninsula and the Kulutingwak Fiord and the Yelverton Inlet (Fig. 1). It is the southern boundary of the Pearya Terrane and represents a suture between the

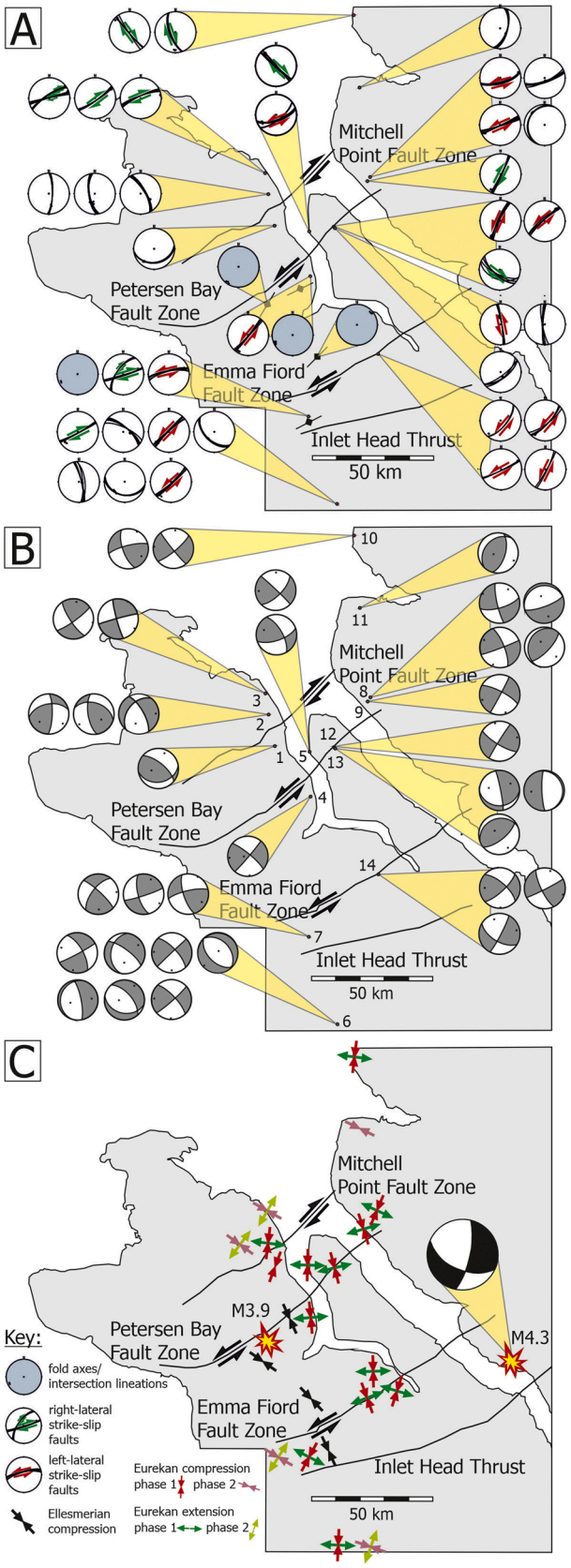

(caption on next column)

Fig. 4. Structural data and fault slip inversion results. A) Stereographic projections of the structural data sets. Left-lateral strike-slip faults are shown in red, right-lateral strike-slip faults in green. Fold axes are plotted as points. B) Result of the fault-slip inversion as P-T-plots. C) Results of the fault slip inversion shown as the orientation of contraction and extension directions. The paleostress field orientation throughout the study area can be subdivided into a NNW-SSE compression (shown in black) that prevailed during the Late Devonian – Early Carboniferous Ellesmerian Orogeny and a roughly N-S compression and a WNW-ESE compression that is related to the Eurekan deformation in the Paleogene.

exotic Pearya Terrane and Laurentia (e.g., Trettin, 1987; Klaper & Ohta, 1993; Piepjohn et al., 2015) (Fig. 1). Outcrops along the fault zone and in the vicinity of the fault were analysed. At the Petersen Bay Fault Zone indicators for left-lateral strike-slip kinematics dominate (Fig. 2A). The faults strike NNE-SSW to NE-SW. A limited number of NW-SE striking right-lateral strike-slip faults, as well as N-S striking normal faults and steep NE-SW striking reverse faults also occur in the outcrops (Fig. 2, B, C, 3).

5.3. *Emma Fiord Fault zone*

The Emma Fiord Fault Zone is located south of the Pearya Terrane in the Franklinian Basin (Figs. 1,4). Directly within the fault zone, left-lateral strike-slip kinematics dominate. Locally, the fault zone is composed of several strike-slip faults, which form a complex cross-cutting pattern (Fig. 5).

5. *4 Faults south of the Emma Fiord Fault zone*

Two outcrops 10 km and 50 km south of the Emma Fiord Fault Zone were analysed (Fig. 4, Table 1). In these outcrops NE-SW striking left-lateral and right-lateral strike-slip faults are exposed.

6. Interpretation of the structural elements

This study and results from previous studies (Piepjohn et al., 2013; Piepjohn & von Gosen, 2017) show that the NE-SW trending Petersen Bay Fault Zone and the Emma Fiord Fault Zone are major faults dominated by left-lateral movements. There are also sub-parallel right-lateral strike-slip faults developed in the study area like the Mitchell Point Fault Zone (Fig. 4A) (Estrada et al., 2006). From the entire fault pattern and the orientation and position of subordinary faults with respect to the main fault, it can be concluded that some differently oriented, subordinate right-lateral strike-slip faults, as documented, e.g., along the Petersen Bay Fault Zone, most-likely represent anti-Riedel shears to the major left-lateral strike-slip faults (Fig. 3). The Eurekan deformation in the study area is characterized by strike-slip tectonics. The northernmost major reverse fault is the Inlet Head Thrust (Piepjohn & von Gosen 2017). Nevertheless, a limited number of normal faults and reverse faults also occur. These faults are exposed, e.g., on the northern part of the peninsula between the Kulutingwak Fiord and the Yelverton Inlet (Fig. 3A). In this location, three different types of faults are developed (strike-slip, normal and reverse faults) (Fig. 2). For a synopsis, the faults are displayed in one stereographic projection (Fig. 3B). Strike-slip faults are shown in black, yellow, and blue. Normal faults in green and reverse faults in red. The comparison of the fault pattern visualized in Fig. 3B with a conceptual kinematic model for a strike-slip fault zone with the related Riedel shears, anti-Riedel shears and the associated normal and reverse faults (Fig. 3C) (the model is based on Wilcox et al., 1973 and Christie-Blick & Biddle, 1985), shows a clear match of the faults developed in the Petersen Bay Fault Zone (Figs. 2, 3B) to the conceptual model for strike-slip zones. The kinematic relationship between the different faults and their orientation imply that these faults likely represent local structural elements that belong to the same strike-slip system, most-likely formed during one deformation phase (Fig. 3).

Table 1
Data base for the fault slip analysis.

Outcrop No.	Outcrop location	Fault kinematics	Fault value pairs	P-axis	T-axis
1	south of Mitchell Point Fault Zone	oblique reverse	5	022/ 19	254/ 61
2	north of Mitchell Point Fault Zone	oblique normal	6	198/ 48	089/ 16
	north of Mitchell Point Fault Zone	oblique reverse	6	234/ 14	126/ 52
	north of Mitchell Point Fault Zone	oblique reverse	3	125/ 17	229/ 40
3	east coast of Wootton Peninsula	right-lateral	4	101/ 03	010/ 16
	east coast of Wootton Peninsula	right-lateral	8	120/ 06	030/ 02
4	south of Petersen Bay Fault zone	left-lateral	4	175/ 05	265/ 09
5	east coast of Kulutingwak Fiord	left-lateral	5	201/ 00	291/ 35
	east coast of Kulutingwak Fiord	right-lateral	4	002/ 14	267/ 18
6	Franklinian Basin	normal	6	030/ 83	226/ 07
	Franklinian Basin	left-lateral	6	180/ 14	273/ 12
	Franklinian Basin	oblique normal	6	183/ 53	058/ 23
	Franklinian Basin	right-lateral	5	288/ 19	194/ 13
	Franklinian Basin	left-lateral	5	182/ 07	274/ 15
	Franklinian Basin	normal	5	267/ 68	035/ 14
	Franklinian Basin	normal	6	250/ 58	084/ 32
7	south of Emma Fiord Fault zone	left-lateral	4	029/ 03	120/ 23
	south of Emma Fiord Fault zone	right-lateral	3	120/ 11	026/ 20
	south of Emma Fiord Fault zone	right-lateral	2	083/ 11	178/ 26
8	north of Petersen Bay Fault zone	left-lateral	5	032/ 21	299/ 06
	north of Petersen Bay Fault zone	normal	5	338/ 59	161/ 31
	north of Petersen Bay Fault zone	left-lateral	5	203/ 09	295/ 13
	north of Petersen Bay Fault zone	thrust	5	129/ 26	325/ 63
9	north of Petersen Bay Fault zone	left-lateral	6	162/ 08	254/ 11
10	north of Hansen Point	right-lateral	3	027/ 06	120/ 26
	north of Hansen Point	right-lateral	4	006/ 11	275/ 05
11	south of Hansen Point	reverse	4	116/ 15	255/ 71
12	Petersen Bay Fault Zone	left-lateral	6	346/ 08	078/ 12
13	Petersen Bay Fault Zone	left-lateral	4	283/ 45	058/ 35
	Petersen Bay Fault Zone	normal	4	091/ 54	266/ 36
	Petersen Bay Fault Zone	reverse	4	146/ 22	310/ 67
14	Emma Fiord Fault Zone	left-lateral	3	178/ 04	270/ 27
	Emma Fiord Fault Zone	left-lateral	2	018/ 13	109/ 07
	Emma Fiord Fault Zone	left-lateral	2	340/ 26	078/ 17

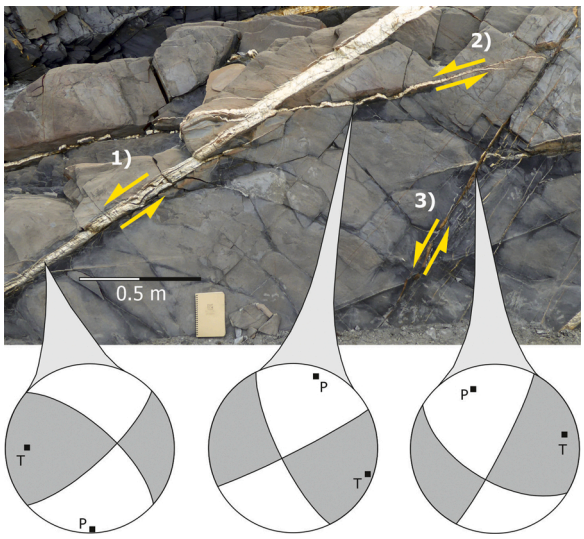

Fig. 5. Outcrop in the Emma Fiord Fault Zone. Different faults are exposed that show left-lateral kinematics. From the cross-cutting relationships it is possible to interpret multiple reactivation phases. The P-T-plot shows the stress field orientations during the different phases. Firstly, NE-SW oriented strike-slip faults formed, then ENE-WSW oriented left-lateral strike-slip faults developed and finally NNE-SSW trending left-lateral strike-slip faults formed. This corresponds to a N-S compression that shifted over NNE-SSW compression/ into a NNW-SSE compression.

This is a little bit different to outcrops within the Emma Fiord Fault Zone, where a multiple reactivation of the major faults due to variations in the paleostress field is indicated. Cross-cutting relationships show that first NE-SW striking left-lateral strike-slip faults formed that were offset by ENE-WSW oriented left-lateral strike-slip faults and finally NNE-SSW trending left-lateral strike-slip faults formed (Fig. 5).

From the slickenside datasets, the P- and T-axes were calculated (Fig. 4B) and the paleostress field orientation was derived (Fig. 4C). In the following, we only refer to the orientation of the paleo-compression. Clearly, paleo-extension occurred orthogonal to this direction. The paleostress field has a relatively even geometry, but minor variations from the general trend occur. The fault-slip inversion indicates two major trends in the orientation of the paleostress field (Fig. 4B). One trend represents a N-S compression that shifted over NNE-SSW compression into a NNW-SSE compression. This temporal evolution can be derived from the Emma Fiord Fault Zone (Fig. 5), where first NE-SW oriented left-lateral strike slip faults were formed, followed by more ENE-WSW oriented left-lateral strike-slip faults and finally NNE-SSW trending left-lateral strike-slip faults occurred. The pattern occurs throughout the study area (Fig. 4C), however, the temporal sequence is derived from the cross-cutting relationships, which are only exposed in the area of the Emma Fiord Fault Zone (Fig. 5).

The second major paleostress field trend that can be derived, is a WNW-ESE compression (Fig. 4C). This trend is also very constant throughout the entire study area.

Southeast of the Petersen Bay Fault Zone, large-scale, NE-SW striking fold structures are developed, which are interpreted as the result of the Ellesmerian Orogeny in the late Paleozoic (e.g., Klaper, 1992; Piepjohn & von Gosen, 2017). The fieldwork carried out so far in this area shows that the occurrence of theses folds is restricted to the area south of the Petersen Bay Fault Zone (Estrada et al., 2006; Piepjohn et al., 2013). In this study we analysed four outcrops with fold structures, where 13 measurements of fold axes and intersection lineations were taken that allow to derive the paleo-shortening in this area. The trend of the analysed fold axes (Fig. 4A) indicates a NW-SE to NNW-SSE compressional stress field in the study area that prevailed throughout the Ellesmerian Orogeny in the Paleozoic (Fig. 4C). This is consistent with previous

studies (Piepjohn et al., 2008, 2013, 2017). The large folds and the related slaty cleavage are Ellesmerian structures and they are unconformably overlain by Paleogene deposits further south at the Hazen Plateau (Piepjohn et al. 2008).

7. Discussion

7.1. Deformation phases

As described above, the paleostress field orientation throughout the study area can be subdivided into three phases: a Paleozoic deformation (NW-SE to NNW-SSE compression), and two Cenozoic phases (a phase with a complex N-S compression followed by WNW-ESE compression) (Fig. 4). The Paleozoic fold structures are the result of the Ellemerian deformation, whereas the Cenozoic strike-slip faults belong to the Eurekan deformation (Piepjohn et al., 2013; Piepjohn & von Gosen, 2017). These two Cenozoic phases are in line with results from Piepjohn et al. (2016), who interpreted the Eurekan deformation as being composed of two phases: a first phase in the early Eocene and a second phase in the late Eocene. Our data indicate that the Eurekan 1 phase was complex and started with N-S compression that subsequently shifted over a NNE-SSW compression into a NNW-SSE compression (Fig. 5). The Eurekan 2 phase is characterized by a simple WNW-ESE compression (Fig. 4B, C). However, it was not possible to resolve the proposed pre-orogenic and post-orogenic phase that was described by Oakey & Chalmers (2012).

7.2. Geodynamic processes and the paleostress field evolution

The Eurekan deformation is attributed to motions of Greenland (e.g., De Paor et al., 1989). In this context, Tessensohn & Piepjohn (2000) developed a three phase - model for the Eurekan deformation. In the first phase, Greenland moved northeastward, and in the second phase, northward movements of Greenland occurred. Subsequently, the Fram Strait opened during the third phase. This model was refined by Piepjohn et al. (2016). During Eurekan phase 1, Greenland moved northward, whereas during Eurekan phase 2 Greenland moved to the WNW (Piepjohn et al., 2016). These directions are reflected by the stress directions that were derived from the slickenside data sets in this study (Fig. 4B, C). During Eurekan phase 1, when the Greenland Plate moved northward, the paleostress field was characterized by a N-S compression that shifted over a NNE-SSW compression into a NNW-SSE compression (Fig. 5, 6A). This is derived from the Emma Fiord Fault Zone, where cross-cutting relationships give evidence for this shift of deformation. During Eurekan phase 2, when the plate vector of Greenland changed and the plate motion was WNW-ward, WNW-ESE compression dominated the area (Fig. 6B). This shows that the paleostress field of northern Ellesmere Island reflects the motions of the Greenland Plate and implies a strong coupling across the Nares Strait that accounts for an effective stress transfer during the Eocene. This observation is supported by the rheology of the lithosphere. Heron et al. (2015) concluded from numerical simulations that the deformed Hazen Stable Block (Fig. 6) has a rather high strength. This may have enhanced the stress transfer into northern Ellesmere Island and would explain the distinct paleostress field that reflects the motion of the Greenland Plate.

7.3. Fault reactivation and timing of deformation

It is common that pre-existing faults undergo a reactivation (e.g., Sibson, 1985). For Andersonian faults, the reactivation potential is strongly controlled by the orientation of the pre-existing fault to the applied principal stresses. The angle between the largest principal stress

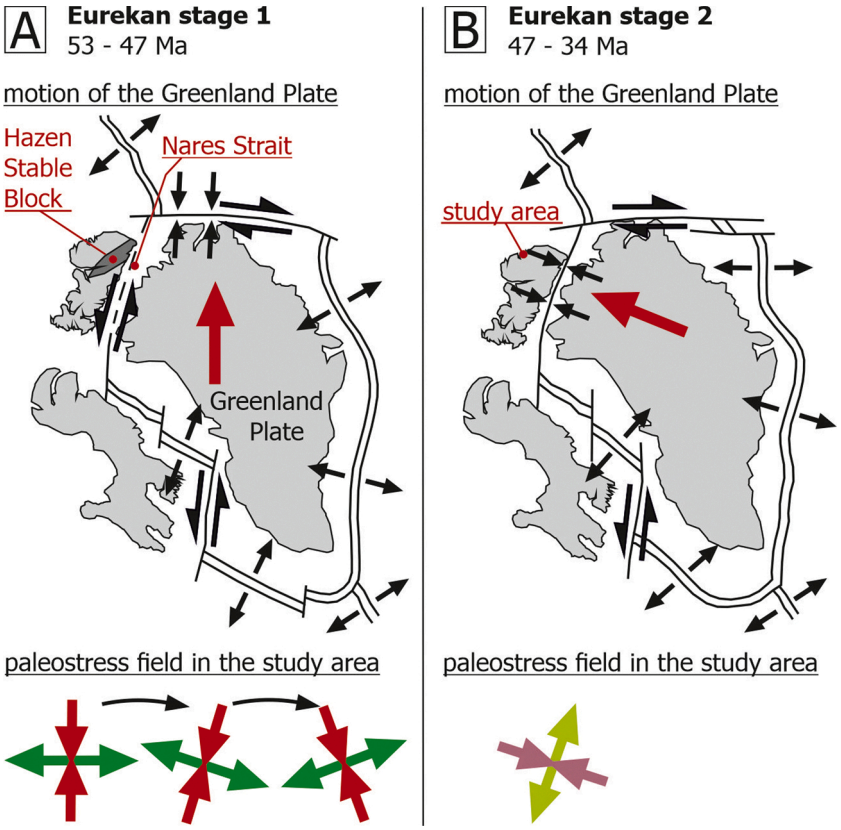

Fig. 6. Motions of the Greenland Plate (based on Tessensohn & Piepjohn, 2000; Piepjohn et al., 2016). Between 53 – 47 Ma, Greenland moved northward causing the roughly N-S compression on northern Ellesmere Island. Between 47 – 34 Ma, the Greenland Plate shifted into a WNW direction, leading to a change in the paleostress field in the study area that was characterized by a WNW-ESE compression at that time.

σ_1 and the fault is named θ. If θ is around 30° the fault is optimally oriented and can be reactivated. The reactivation potential decreases with an increase of θ. For 2θ no reactivation is possible (Sibson, 1985). In this study we use the P- and T-axes method for the paleostress field analysis, based on the approach of Marrett & Allmendinger (1990). The P- and T-axes may, but do not have to match with the principal stresses σ_1 and σ_3 (Allmendinger, 1989). According to Allmendinger (1989), in a P-T-plot, σ_1 is located within the P-quadrant and σ_3 in the T-quadrant and provides a reliable indication for the paleostress field. In case of co-axial deformation, the P- and T-axes coincide with the principal stress axes (Peresson & Decker, 1997). Therefore, the orientations of the P- and T-axes with respect to the fault plane, deliver a suitable proxy for the fault reactivation potential.

Many of the Eurekan faults along the southeastern boundary and southeast of the Pearya Terrane (Fig. 1) are interpreted as reactivated Ellemerian structures (Piepjohn et al., 2013). On Fig. 4C, the direction of compression during the Ellesmerian Orogeny (black arrows) is shown, based on fold axis orientations measured in the field (Fig. 4A). The Ellesmerian paleostress field was NW-SE to NNW-SSE oriented, which can have produced NE-SW striking reverse faults and thrusts (Fig. 7A). Data from the Emma Fiord Fault Zone implies that such NE-SW trending faults could have been later reactivated as left-lateral strike-slip faults during the NNE-SSW directed Eurekan phase 1 compression (Fig. 7B), when the angle between the P-axis and the fault plane was about 44°. The possible subsequent shift of the paleostress field into a NNW-SSE compression could have stopped the activity of these faults (Fig. 7B).

Left-lateral strike-slip kinematics dominate at the NE-SW-striking major faults, e.g., at the Petersen Bay Fault Zone (Fig. 2) and the Emma Fiord Fault Zone. Major NW-SE striking faults are not developed. Some minor NW-SE-striking right-lateral strike-slip faults represent anti-Riedel shears of the major NE-SW left-lateral strike-slip faults (Fig. 3). However, also the major NE-SW faults show right-lateral kinematics, like the Mitchell Point Fault Zone, the Petersen Bay Fault Zone and the Emma Fiord Fault Zone (Estrada et al., 2006; Piepjohn et al., 2013), and it has been previously postulated that the left-lateral strike-slip faults represent the first phase of movements and the right-lateral strike-slip faults represent the second phase of movements during the Eurekan deformation (Piepjohn et al., 2016). This hypothesis is supported by the paleostress field analysis of this study (Fig. 4). As described above, the paleostress field can be subdivided into two phase stages, the Eurekan phase 1 and phase 2 deformation. Pre-existing NE-SW Ellesmerian faults were prone for left-lateral slip under NNE-SSW compression that prevailed during the Eurekan phase 1 (Fig. 7B). When the stress field shifted into NNW-SSE compression, fault activity stopped. Right-lateral movements were likely possible later along these faults under a WNW-ESE compression that acted during Eurekan phase 2 (Fig. 7C). In this case, the angle between the P-axis and the fault plane was again in the range of 44° that allowed a reactivation. This implies that the left-lateral fault activity was likely older than the right-lateral fault activity and supports the assumption that the Eurekan phase 1 deformation is characterized by left-lateral strike-slip faults, whereas during Eurekan phase 2 the majority of right-lateral strike-slip faults formed.

7.4. Recent seismicity

In 1998 an earthquake was recorded in the study area with a magnitude of 4.3 (Bent & Perry, 1999). The calculated epicenter was located south of the Emma Fiord Fault Zone (Fig. 4C). Another seismic event with a magnitude of 3.9 took place in 2001 (https://earthquake.usgs.gov). The epicenter of this earthquake was very close to the Petersen Bay Fault Zone (Fig. 4C). The fault plane solution of the 1998 earthquake shown in Bent & Perry (1999), indicates strike-slip kinematics with a normal fault component related either to a steep NNE-SSW striking fault or a slightly less steep dipping WNW-ESE striking fault surface (Fig. 4C). From the field data it is evident that oblique faulting with a strike-slip component was characteristic for the Eurekan deformation phase in the Paleogene. The fault plane solution of the M4.3 earthquake also shows oblique strike-slip kinematics. This implies that strike-slip fault activity still occurs in this area, today. From the fault plane solution, a recent stress field can be derived, which is characterized by NNW-SSE compression. The epicenter location of the 2001 earthquake close to the Petersen Bay Fault Zone, indicates that this major fault zone experienced activity over the last 350 Myr (Ellesmerian, Eurekan and Recent). Though the database of the recent seismicity is very limited so far, it allows to derive that individual faults on northern Ellesmere Island are still active or undergo a reactivation. The recent earthquakes indicate that some of the Eurekan faults are optimally oriented for a reactivation under the current regional stress field. However, there is the possibility that the fault activity might be also related to stress field changes that are caused by the volume loss of glaciers. Different studies show that the glaciers in the Canadian Arctic have a negative balance and undergo a volume loss (Koerner, 2005; Fisher et al., 2012; White & Copland, 2019). Changes in the ice thickness produce significant stress changes in the lithosphere and thus can have an influence on the seismicity (Cohen, 1993). This effect has been, e.g., documented for glaciers in Alaska (Doser et al., 2007; Masih, 2018).

This study supports the previous assumption that the Eurekan deformation was a complex tectonic event, which was controlled by the three ocean system (Labrador Sea – Baffin Bay, North Atlantic and Eurasian Basin) around the Greenland Plate (e.g., Piepjohn et al., 2016). Our structural data set shows that the Eurekan phase 1 was characterized by N-S compression that shifted to NNE-SSW compression and later to NNW-SSE compression. We do not treat these variations in the shortening direction as separate phases, because the directions of compression are not significantly different. Nevertheless, they might represent some minor changes in movement of the Greenland Plate, but this remains speculative. The fact that the movement of the Greenland Plate was manifested in the structural elements of northern Ellesmere

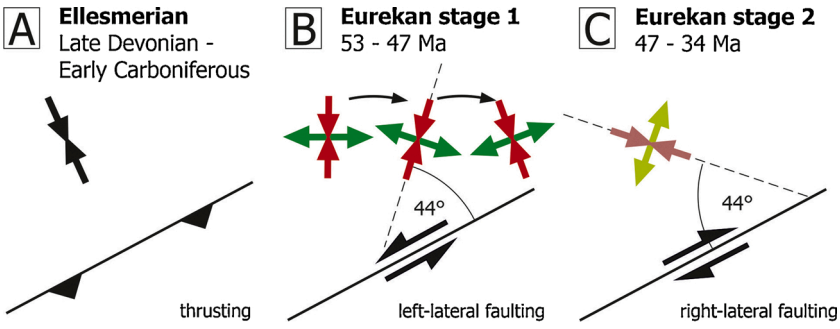

Fig. 7. Timing for faulting: A) Under a NW-SE direction compression, NE-SW oriented faults formed during the Ellesmerian Orogeny. B) Eurekan phase 1 with NNE-SSW compression that led to left-lateral movements on the pre-existing faults. C) Eurekan phase 2 with WNW-ESE compression that caused right-lateral movements on the pre-existing faults.

Island implies a strong coupling between Greenland and Ellesmere Island.

7.5. Limitations of the analyses

The applied kinematic analysis of the fault data was performed with the approach of Marrett & Allmendinger (1990), which is very robust. The concept behind a fault-slip analysis is the Wallace-Bott hypothesis, which means that the slip along a fault occurs parallel to the maximum resolved shear stress on the fault surface (Wallace, 1951; Bott, 1959). The Wallace-Bott hypothesis requires that the faults are planar, the fault blocks behave rigidly, the applied stress is uniform and no stress perturbations and block rotations occur along the fault surface (Pascal, 2002). We assume that these requirements are fulfilled for the analysed outcrops. However, there are always additional uncertainties that arise from a post-fault rotation of the outcrops, the sampling strategy and the spatial homogeneity of the strain (Marrett & Allmendinger, 1990). The logistics and the outcrop conditions only allowed to take a limited number of measurements for each fault surface. Nevertheless, these measurements are representative and reflect the kinematics of the faults. It has been shown that stress inversion techniques are valid, if the slip direction is controlled by the orientation of the fault surface and a homogeneous regional stress field (Pollard et al., 1993). The results imply that the paleostress field was homogenous (Fig. 4C). The consistent orientation of the paleostress field throughout the study area (Fig. 4C) indicates that the data set is robust and the related derivations are rational.

8. Conclusions

The paleostress field based on fold axes and slickenside data shows that the study area was affected by at least three tectonic deformation phases, 1) the Ellesmerian (NW-SE compression), the Eurekan phase 1 (left-lateral strike-slip faulting/N-S compression) and the Eurekan phase 2 (right-lateral strike-slip faulting/WNW-ESE compression). The deformation of northern Ellesmere Island is largely controlled by the northwestward stress transfer from the Greenland Plate and implies a significant coupling across the Nares Strait. The paleostress field analysis is consistent with the assumption that the Eurekan strike-slip faults southeast of the Pearya Terrane are reactivated Ellesmerian structures. The left-lateral strike-slip fault activity was likely older than the right-lateral strike-slip fault activity. This supports the assumption that the Eurekan phase 1 deformation on Ellesmere Island is characterized by left-lateral strike-slip faults, whereas during Eurekan phase 2 the majority of right-lateral strike-slip faults formed. Ongoing seismic activity in the area of the Pearya Terrane and southeast of it implies that some of the faults in this region are still active.

Author statement

All authors contributed to the manuscript and agree with the current version.

Declaration of Competing Interest

The authors report no declarations of interest.

Acknowledgements

The German Research Foundation (DFG) is gratefully acknowledged for funding Christian Brandes (project BR 3779/3-1). Fieldwork conducted under the CASE 19-expedition in 2017 would not have been feasible without support of the following organizations: Hamlets of Grise Fiord and Resolute Bay, Hunters and Trappers Associations of Grise Fiord and Resolute Bay, Nunavut Impact Review Board, Nunavut Planning Commission, Nunavut Research Institute, Nunavut Water Board and the Qikiqtani Inuit Association. We are grateful to the Canadian Polar Continental Shelf Program (PSCP) for the excellent logistic support. The fieldwork would not have been possible without the people who organized the expeditions and were responsible for the safety of the expedition members: special thanks go to Christoph Kasch for his logistic and technical support and to the cook, wildlife monitors, pilots and engineers. We are grateful to Thomas Plenefisch for discussion. Three anonymous reviewers are gratefully acknowledged for their constructive comments.

References

Allmendinger, R.W., 1989. Notes on fault slip analysis. Prepared for the Geological Society of America Short Course on “Quantitative Interpretation of Joints and Faults” November 4 & 5, 1989, with contributions of Gephart, J.W. and Marrett, R. A., p. 56.

Arbeitskreis Geologie und Geophysik der Polargebiete der Deutschen Gesellschaft für Polarforschung (AGGP), 2015. Geowissenschaftliche Polarforschung in Deutschland – globale Bedeutung und Perspektiven. Polarforschung 85, 1–64.

Bent, A.L., Perry, C., 1999. Focal mechanisms for eastern Canadian earthquakes: 1 January 1996 – 30 June 1998. Geological Survey of Canada, p. 148. Open File 3698.

Beranek, L.P., Pease, V., Hadlari, T., Dewing, K., 2015. Silurian flysch successions of Ellesmere Island, Arctic Canada, and their significance to northern Caledonian palaeogeography and tectonics. Journal of the Geological Society 172, 201–212.

Bjørnerud, M.G., Bradley, D.C., 1994. Silurian foredeep and accretionary prism in northern Ellesmere Island: implications for the nature of the Ellesmerian Orogen. In: Thurston, D., Fujita, K. (Eds.), Proceedings of the 1992 International Conference on Arctic Margins. . OCS Study MMS 94-0040, pp. 129–133.

Bott, M.H.P., 1959. The mechanics of oblique slip faulting. Geological Magazine 96, 109.

Christie-Blick, N., Biddle, K.T., 1985. Deformation and Basin Formation along Strike-Slip Faults. In: Biddle, K.T., Christie-Blick, N. (Eds.), Strike-Slip deformation, basin formation and sedimentation, Society of Economic Paleontologists and Mineralogists, 37. Special Publications, pp. 1–34.

Churkin, M., Trexler, J.H., 1980. Circum-Arctic plate accretion – isolating part of a Pacific plate to form the nucleus of the Arctic basin. Earth and Planetary Science Letters 48, 356–362.

Cohen, S.C., 1993. Does rapid change in ice loading modulate strain accumulation and release in glaciated, tectonically active regions. Geophysical Research Letters 20, 2123–2126.

Delvaux, D., Moeys, R., Stapel, G., Petit, C., Levi, K., Miroshnichenko, A., Ruzhich, V., San’kov, V., 1997. Paleostress reconstructions and geodynamics of the Baikal region, Central Asia, Part 2. Cenozoic rifting. Tectonophysics 282, 1–38.

De Paor, D.G., Bradley, D.C., Eisenstadt, G., Phillips, S.M., 1989. The Arctic Eurekan orogen: A most unusual fold-and-thrust belt. Geological Society of America Bulletin 101, 952–967.

Dewing, K., Harrison, J.C., Pratt, B.R., Mayr, U., 2004. A probable late Neoproterozoic age for the Kennedy Channel and Ella Bay formations, northeastern Ellesmere Island and its implications for passive margin history of the Canadian Arctic. Canadian Journal of Earth Sciences 41, 1013–1025.

Dewing, K., Mayr, U., Harrison, J.C., de Freitas, T., 2008. Upper Neoproterozoic to Lower Devonian stratigraphy of northeast Ellesmere Island. In: Mayr, U. (Ed.), Geology of northeast Ellesmere Island adjacent to Kane Basin and Nares Strait, 592. Geological Survey of Canada Bulletin, pp. 31–108.

Dewing, K., Hadlari, T., Pearson, D.G., Matthews, W., 2019. Early Ordovician to Early Devonian tectonic development of the northern margin of Laurentia, Canadian Arctic Islands. GSA Bulletin 131, 1075–1094.

Doser, D.I., Wiest, K.R., Sauber, J., 2007. Seismicity of the Bering Glacier region and its relation to tectonic and glacial processes. Tectonophysics 439, 119–127.

Estrada, S., Henjes-Kunst, F., 2013. ^{40}Ar-^{39}Ar and U-Pb dating of Cretaceous continental rift-related magmatism on the northeast Canadian Arctic margin. German Journal of Geosciences (Zeitschrift der Deutschen Gesellschaft für Geowissenschaften) 164, 107–130.

Estrada, S., Piepjohn, K., Henjes-Kunst, F., von Gosen, W., 2006. Geology, magmatism and structural evolution of the Yelverton Bay area, northern Ellesmere Island, Arctic Canada. Polarforschung 73, 59–75.

Fisher, D., Zheng, J., Burgess, D., Zdanowicz, C., Kinnard, C., Sharp, M., Bourgeois, J., 2012. Recent melt rates of Canadian arctic ice caps are the highest in four millennia. Global and Planetary Change 84-85, 3–7.

Frisch, T., 1974. Metamorphic and plutonic rocks of northernmost Ellesmere Island, Canadian Arctic Archipelago. Geological Survey of Canada Bulletin 229, 1–87.

Gion, A.M., Williams, S.E., Müller, R.D., 2017. A reconstruction of the Eurekan Orogeny incorporating deformation contraints. Tectonics 36, 304–320.

Hadlari, T., Davis, W.J., Dewing, K., 2014. A pericratonic model for the Pearya terrane as an extension of the Franklinian margin of Laurentia, Canadian Arctic. Geological Society of America Bulletin 126 (1–2), 182–200 doi.10.1130/B30843.1.

Heron, P.J., Pysklywec, R.N., Stephenson, R., 2015. Intraplate orogenesis within accreted and scarred lithosphere: Example of the Eurekan Orogeny, Ellesmere Island. Tectonophysics 664, 202–213. https://doi.org/10.1016/j.tecto.2015.09.011.

Klaper, E.M., 1992. The Paleozoic tectonic evolution of the northern edge of North America: A structural study of northern Ellesmere Island, Canadian Arctic Archipelago. Tectonics 11, 854–870.

Klaper, E.M., Ohta, Y., 1993. Paleozoic metamorphism across the boundary between the Clements Markham fold belt und the Pearya terrane in northern Ellesmere Island, Canadian Arctic Archipelago. Canadian Journal of Earth Sciences 30, 867–880.
Koerner, R.M., 2005. Mass balance of glaciers in the Queen Elizabeth Islands, Nunavut, Canada. Annals of Glaciology 42, 417–423.
Lacombe, O., 2012. Do fault slip data inversions actually yield 'paleostresses' that can be compared with contemporary stresses? A critical discussion. Comptes Rendus Geoscience 344, 159–173. https://doi.org/10.1016/j.crte.2012.01.006.
Lepvrier, C., 1990. Early Tertiary paleostress history and tectonic development of the Forlandsundet Basin, Svalbard. Norway. Meddelelser 112, 1–16.
Lepvrier, C., 1992. Early Tertiary paleostress distribution on Spitsbergen: implications for the tectonic development of the western fold-and-thrust belt. Nor. Geol. Tidsskr. 72, 129–135.
Lepvrier, C., Geyssant, J., 1984. Tectonique cassante et champs de contrainte tertiaires le long de la marge en coulissement du Spitsberg: Corrélations avec les mécanismes d'ouverture de la mer de norvège-Gröenland. Ann. Soc. Geol. Nord, III 333–344.
Malone, S.J., 2012. Tectonic evolution of northern Ellesmere Island: insights from the Pearya Terrane. Ellesmerian Clastic Wedge and Sverdrup Basin. University of Iowa, p. 276. PhD thesis.
Marrett, R., Allmendinger, R.W., 1990. Kinematic analysis of fault-slip data. Journal of Structural Geology 12, 973–986.
Masih, A., 2018. An enhanced seismic activity observed due to climate change: preliminary results from Alaska. In: IOP Conference Series: Earth and Environmental Sciences, 167, p. 012018. https://doi.org/10.1018/1755-1315/167/1/012018.
McClelland, W.C., Malone, S.J., von Gosen, W., Piepjohn, K., Läufer, A., 2012. The timing of sinistral displacement of the Pearya Terrane along the Canadian Arctic margin. German Journal of Geosciences (Zeitschrift der Deutschen Gesellschaft für Geowissenschaften) 163, 251–259.
Oakey, G.N., Chalmers, J.A., 2012. A new model for the Paleogene motion of Greenland relative to North America: Plate reconstructions of the Davis Strait and Nares Strait regions between Canada and Greenland. Journal of Geophysical Research 117, B10401. https://doi.org/10.1029/2011JB008942.
Pascal, C., 2002. Interaction of faults and perturbation of slip: influence of anisotropic stress states in the presence of fault friction and comparison between Wallace–Bott and 3D distinct element models. Tectonophysics 356, 307–322.
Peresson, H., Decker, K., 1997. The Tertiary dynamics of the northern Eastern Alps (Austria): changing paleostresses in a collisional plate boundary. Tectonophysics 272, 125–157.
Piepjohn, K., Tessensohn, F., Harrison, C., Mayr, U., 2000. Involvement of a Tertiary Foreland Basin in the Eurekan Foldbelt Deformation, NW Coast of Kane Basin, Ellesmere Island. Canada. Polarforschung 68, 101–110.
Piepjohn, K., von Gosen, W., Läufer, A., McClelland, W.C., Estrada, S., 2013. Ellesmerian and Eurekan fault tectonics at the northern margin of Ellesmere Island (Canadian High Arctic). German Journal of Geosciences (Zeitschrift der Deutschen Gesellschaft für Geowissenschaften) 164, 81–105.
Piepjohn, K., von Gosen, W., 2017. Structural transect through Ellesmere Island (Canadian Arctic): superimposed Palaeozoic, Ellesmerian and Cenozoic Eurekan deformation. In: Pease, V., Coakley, B. (Eds.), Circum-Arctic Lithosphere Evolution, 460. Geological Society, London, pp. 33–56. Special Publications.
Piepjohn, K., von Gosen, W., Tessensohn, F., 2016. The Eurekan deformation in the Arctic: an outline. Journal of the Geological Society of London 173, 1007–1024. https://doi.org/10.1144/jgs2016-081.
Piepjohn, K., von Gosen, W., Tessensohn, F., Reinhardt, L., McClelland, W.C., Dallmann, W., Gaedicke, C., Harrison, J.C., 2015. Tectonic map of the Ellesmerian and Eurekan deformation belts on Svalbard, North Greenland, and the Queen Elizabeth Islands (Canadian Arctic). Arktos 1. https://doi.org/10.1007/s41063-015-0015-7.
Piepjohn, K., von Gosen, W., Tessensohn, F., Saalmann, K., 2008. Ellesmerian fold-and-thrust belt (northeast Ellesmere Island, Nunavut) and its Eurekan overprint. In: Mayr, U. (Ed.), Geology of northeast Ellesmere Island adjacent to Kane Basin and Nares Strait, 592. Geological Survey of Canada Bulletin, pp. 285–303.
Pollard, D.D., Saltzer, S.D., Rubin, A.M., 1993. Stress inversion methods: are they based on faulty assumptions? Journal of Structural Geology 15, 1045–1054.
Saalmann, K., Tessensohn, F., Piepjohn, K., von Gosen, W., Mayr, U., 2005. Structure of Palaeogene sediments in east Ellesmere Island: Constraints on Eurekan tectonic evolution and implications for the Nares Strait problem. Tectonophysics 406, 81–113.
Saalmann, K., Tessensohn, F., von Gosen, W., Piepjohn, K., 2008. Structural evolution of Tertiary rocks on Judge Daly Promontory. In: Mayr, U. (Ed.), Geology of northeast Ellesmere Island adjacent to Kane Basin and Nares Strait, 592. Geological Survey of Canada Bulletin, pp. 305–323.
Saintot, A., Angelier, J., 2002. Tectonic paleostress fields and structural evolution of the NW-Caucasus fold-and-thrust belt from Late Cretaceous to Quaternary. Tectonophysics 357, 1–31.
Schuchert, C., 1923. Sites and nature of North American geosynclines. Bulletin of the Geological Society of America 34, 151–229.
Sibson, R.H., 1985. A note on fault reactivation. Journal of Structural Geology 7, 751–754.
Stephenson, R., Piepjohn, K., Schiffer, C., von Gosen, W., Oakey, G.N., Anudu, G., 2017. Integrated crustal-geological cross-section of Ellesmere Island. In: Pease, V., Coakley, B. (Eds.), Circum-Arctic Lithosphere Evolution, 460. Geological Society Special Publication, London, pp. 7–17.
Tessensohn, F., Piepjohn, K., 2000. Eocene Compressive Deformation in Arctic Canada, North Greenland and Svalbard and Its Plate Tectonic Causes. In: Polarforschung 68. In: Roland, N.W., Tessensohn, F. (Eds.), ICAM III – International Conference on Arctic Margins, Vol. I, pp. 121–124.
Thorsteinsson, R., Tozer, E.T., 1970. Geology of the Arctic Archipelago. In: Douglas, R.J. W. (Ed.), Geology and economic minerals of Canada. Geological Survey Canada, Economic Geology Report 1, pp. 547–590.
Trettin, H.P., 1987. Pearya: a composite terrane with Caledonian affinities in northern Ellesmere Island. Canadian Journal of Earth Sciences 24, 224–245.
Trettin, H.P., 1991. The Proterozoic to Late Silurian record of Pearya. In: Trettin, H.P. (Ed.), Chapter 9 in Geology of the Innuitian Orogen and Arctic Platform of Canada and Greenland. Geological Survey of Canada 3, pp. 239–260.
Trettin, H.P., Frisch, T., 1987. Bedrock geology, Yelverton Inlet map-area, northern Ellesmere Island. Geological Survey of Canada Open File, p. 98.
Trettin, H.P., Frisch, T., 1996. Geology, Yelverton Inlet, District of Franklin, Northwest Territories. Geological Survey of Canada. Map 1881A, scale 1:250 000.
Trettin, H.P., Parrish, R., 1987. Late Cretaceous bimodal magmatism, northern Ellesmere Island: isotopic age and origin. Canadian Journal of Earth Sciences 24, 257–265.
Von Gosen, W., Piepjohn, K., McClelland, W.C., Läufer, A., 2012. The Pearya shear zone in the Canadian High Arctic: kinematics and significance. German Journal of Geosciences (Zeitschrift der Deutschen Gesellschaft für Geowissenschaften) 163, 233–249.
Wallace, R.E., 1951. Geometry of shearing stress and relation to faulting. The Journal of Geology 59, 118–130.
Wilcox, R.E., Harding, T.P., Seely, D.R., 1973. Basic wrench tectonics. American Association of Petroleum Geologists Bulletin 57, 74–96.
White, A., Copland, L., 2019. Loss of floating glacier tongues from the Yelverton Bay region, Ellesmere Island. Canada. Journal of Glaciology 65, 376–394.